Title
Hydraulic modeling of the 2011 New Madrid Floodway activation: a case study on floodway activation controls

Journal
Natural Hazards, 77(3)

ISSN
0921-030X

Authors
Luke, Adam
Kaplan, Brad
Neal, Jeff
et al.

Publication Date
2015-07-01

DOI
10.1007/s11069-015-1680-3

Peer reviewed

Nat Hazards (2015) 77:1863–1887
DOI 10.1007/s11069-015-1680-3

ORIGINAL PAPER

Hydraulic modeling of the 2011 New Madrid Floodway activation: a case study on floodway activation controls

Adam Luke[1,2] · Brad Kaplan[2] · Jeff Neal[3] · Jeremiah Lant[2] · Brett Sanders[1] · Paul Bates[3] · Doug Alsdorf[2]

Received: 27 August 2014 / Accepted: 28 February 2015 / Published online: 8 March 2015

Abstract Engineered floodways are floodplains managed by hydraulic controls that can be activated passively, whereby the floodway fills and empties with changes in channel stage, or through a rapid control action, such as the detonation of a levee. During May of 2011, the Birds Point-New Madrid Floodway (NMF) was activated through levee detonation and the performance of this approach is examined herein. A two-dimensional hydraulic flood model (LISFLOOD-FP) is applied to the NMF and calibrated for April and May of 2011 in order to recreate the levee detonation scenario (detonation control). Additionally, the model is applied to simulate flood impacts had the NMF been activated passively, without the deliberate breaching of the levees (passive control). Results show that detonation control reduced flood stages upstream of the activation site by 0.8 m (2.62 ft) without significantly altering overall flooding extent compared with the passive control scenario. Damage estimates from the US Federal Emergency Management Agency HAZUS-MH model indicate that detonation control slightly reduced losses associated with building replacement costs and damaged crops (4.0 % reduction). However, floodway and levee damages that occurred under the detonation control required over 50 million US$ in repairs, and these costs would have been greatly reduced under a passive control scenario. These results indicate that the detonation control effectively reduced flood stage and the risk of upstream levee failures without increasing flooding extent, building losses, and crop damages, but the potential for floodway erosion and deposition deserves additional consideration in the implementation of a rapid activation design.

✉ Adam Luke
aluke1@uci.edu

[1] Department of Civil and Environmental Engineering, University of California, Irvine, CA 92617, USA

[2] Byrd Polar Research Center, The Ohio State University, Columbus, OH 43201, USA

[3] School of Geographical Sciences, University of Bristol, Bristol, UK

Keywords Hydraulic modeling · Floodway activation · Flood damages · New Madrid Floodway · Cairo · Levee detonation

1 Introduction

Managing riverine and coastal flooding is a long-standing and growing challenge. The total global exposure to flooding has been estimated at 46 trillion US$ in 2010 and is expected to grow to 158 trillion US$ by 2050 based on trends in population density and GDP per capita (Jongman et al. 2012). In the USA, large-scale flooding events like the 2011 Mississippi River floods have caused approximately 8.2 billion US$ in damages and 89 fatalities per year for the past 30 years according to flood loss data from the National Oceanic and Atmospheric Administration's Hydrologic Information Center. One of the more promising approaches to managing riverine flood risk is the use of engineered floodways, because in addition to providing flood storage and conveyance which help to attenuate floods, benefits are offered to fisheries, wetlands, wildlife, and agriculture (Sommer et al. 2001). Engineered floodways are parts of the floodplain that can be activated during an extreme event to store and convey flood water. Floodways provide additional services such as agricultural production and wildlife habitat at other times. Examples in North America include the Yolo and Sutter Bypasses near Sacramento, California, the Red River Floodway near Winnepeg, Canada, the Morganza Floodway near Morganza, Louisiana, and the Birds Point-New Madrid Floodway (NMF) near Cairo, Illinois. Floodways mimic the natural hydraulic function of the floodplain relative to flood storage and conveyance while being responsive to engineering controls such as gates, weirs, and deliberate levee breaches to enable management for multiple beneficial uses (Kelley 1998).

Hydraulic controls during extreme events have a profound effect on flood impacts. Hydraulic flow theory suggests that the diversion of channel flows into the floodplain through a breach acts to lower flood stage both upstream and downstream of the diversion location by creating depression waves that propagate away from the diversion location with an amplitude and length that is commensurate with the diversion rate and duration, respectively (Sanders and Katopodes 1999a, b, 2000). Additionally, a rapid control action such as the sudden opening of a gate or the deliberate breaching of a levee can create larger diversion rates and thus larger depression wave amplitudes and channel stage reductions than are possible with passive control alternatives, whereby the floodplain gradually fills and empties with changes in channel stages (Sanders et al. 2006). On the other hand, a rapid control action may be ineffective if it is ill-timed because the depression waves generated in the channel may be out of phase with the peak of the flood (Jaffe and Sanders 2001; Sanders et al. 2006). A rapid control action can also lead to high-velocity breach flows that can cause significant erosion and deposition, which is damaging to floodplains (Londono and Hart 2013). Due to the complexity of operational floodways, which are subject to uncertain inflows based on meteorological and hydrological forcing, as well as management policies that demand strict adherence, it is challenging to optimize the performance of the system for multiple benefits.

In April and May of 2011, the Mississippi River basin experienced record levels of flooding, which prompted the US Army Corps of Engineers (USACE) to activate the NMF located approximately 200 km (125 mi) south of St. Louis in Mississippi County and New Madrid County, Missouri. The NMF was designed to provide emergency flood relief for

Cairo, Illinois, located at the confluence of the Mississippi and Ohio Rivers and immediately upstream of the NMF (Fig. 1). The NMF was activated by detonating explosives placed at strategic levee locations (Fig. 2). Just 7 h after detonation at the northern fuseplug, flood stage at Cairo was 0.3 m (1 ft) lower than flood stage prior to detonation, which clearly helped to protect the city from flooding (Koenig and Holmes Jr 2013). Approximately 53,000 ha (130,000 ac) of farmland in the NMF were inundated, and the high-velocity breach flows caused significant floodplain erosion and deposition (Londono and Hart 2013).

In this paper, a two-dimensional (2D) hydraulic flood model (LISFLOOD-FP) is applied to the NMF and calibrated for April and May of 2011 using available river and floodway gage measurements, flood extent data, and records of control actions. Model results are analyzed to measure changes in river flood stages, the extent of floodplain inundation, potential floodplain erosion, and flood damages using the HAZUS-MH model (Scawthorn et al. 2006). Additionally, the model is applied to simulate the likely flood impacts had the NMF been operated passively, i.e., without the deliberate breaching of levees. The methodology used to compare the effectiveness of these two flood protection measures is similar to the methodology outlined by Ernst et al. (2010), although in this study, the social impacts are ignored and the scale is regional instead of micro. To date, there has been little work done to analyze the performance of floodways from a hydraulic control perspective, and the objective of this paper was to better understand how flood attributes in general, and damages in particular, would have differed as a consequence of the hydraulic controls. This study points to significant flood management benefits from both active and passive use of the floodplain, as well as tradeoffs between passive and active control scenarios, which deserve careful consideration in the context of future flood management decision-making.

2 Site description

Due to Cairo's location at the confluence of the Ohio and Mississippi Rivers, the city experiences a high level of flood risk. Cairo has the lowest elevation of any city within Illinois and is the only city in the state completely surrounded by levees. The Great

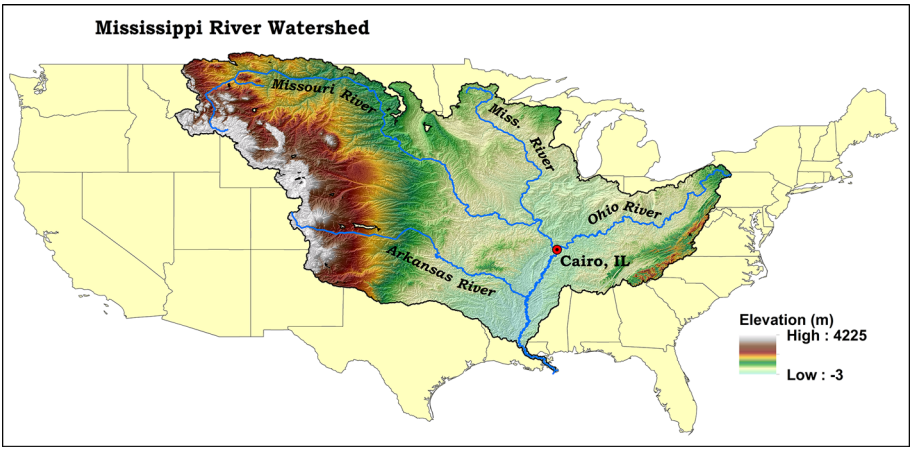

Fig. 1 Mississippi River Watershed and the location of Cairo, Illinois, at the confluence of the Ohio and Mississippi Rivers

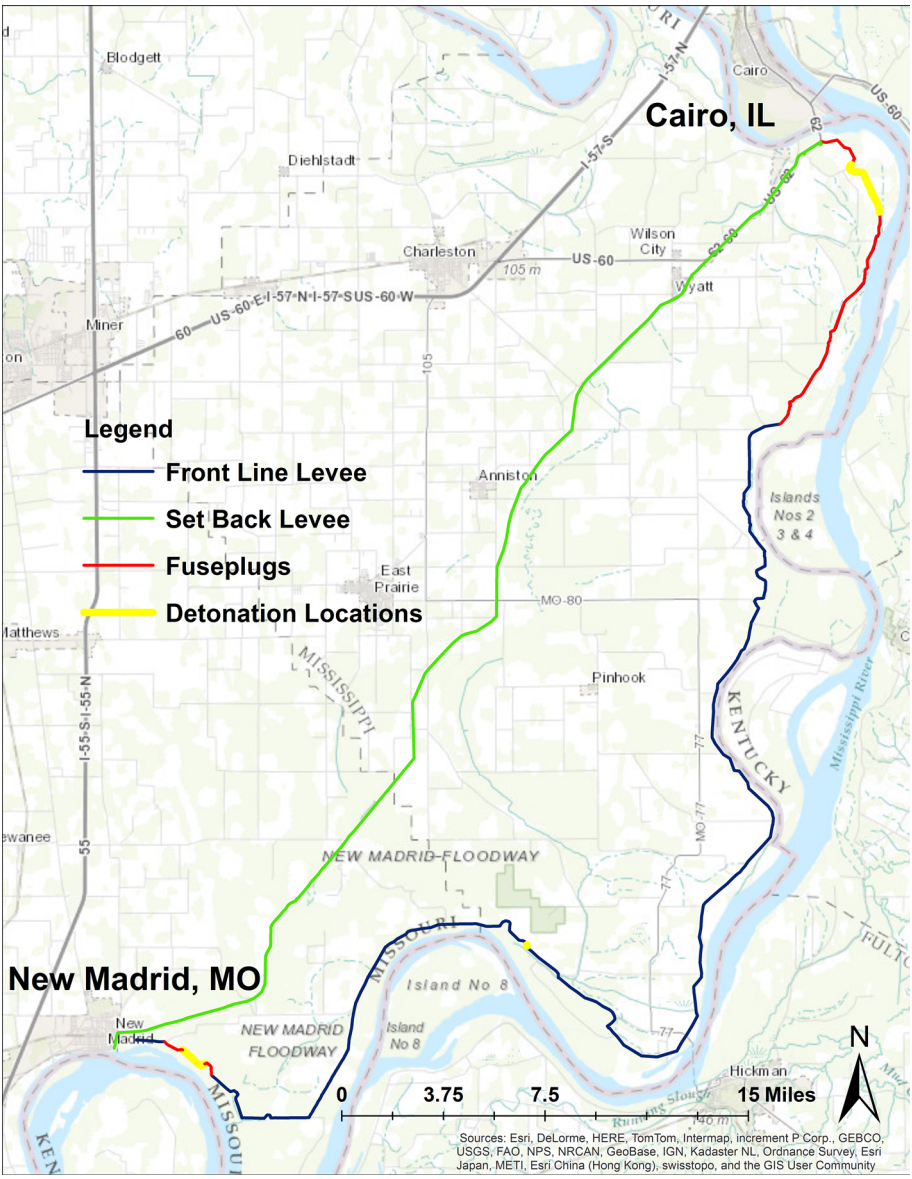

Fig. 2 Schematic of the Bird's Point-New Madrid Floodway

Mississippi Flood of 1927 led to the strengthening of the levee system around Cairo and the construction of the NMF (USACE 2010).

The construction of the NMF began in October of 1929 in response to the Flood Control Act of 1928, which authorized the USACE to design and construct projects for flood control on the Mississippi River. The floodway consists of a 90-km (56 mi) front line levee on the east and a 58-km (36 mi) set back levee on the west (Fig. 2). The front line levee stretches from Birds Point, Missouri, to New Madrid, Missouri, and serves to constrain

flood waters to the Mississippi River, while the set back levee serves to contain water within the floodway if the floodway is activated (USACE 2010). There is a 460-m (1500 ft) gap between the front line and set back levees at the south-western corner of the floodway, which permits backwater flooding of the lower area of the floodway. The front line levee contains two sections that were constructed at a lower elevation than adjacent sections. These "fuseplug" sections are 18 km (11 mi) and 8 km (5 mi) long and are located south of Cairo and east of New Madrid, respectively. The floodway is activated when these fuseplug sections are naturally overtopped (passive control) or artificially crevassed by detonating an explosive charge (detonation control) (USACE 2010).

Two flooding events have led to the detonation of the front line levee. The first was during The Great Flood of 1937, when record flood discharges from the Ohio River caused the highest flood stages recorded to date at Cairo. This prompted multiple detonations at the northern fuseplug, which successfully diverted flood discharge into the floodway. The second activation occurred on May 2, 2011, when stage recorded at the Ohio River gage at Cairo reached a new record level of 101.36 m (332.55 ft) above NAVD88 (USACE 2010). Three levee detonations were executed, which allowed for floodwaters to enter the floodway and then return to the channel at the lower section of the floodway. The first detonation took place at 10:03 pm on May 2, 2011, which breached a 3.2-km (2 mi) stretch of the northern fuseplug. The detonation caused a 0.15-m (0.5 ft) reduction in stage within the first hour compared with stage prior to detonation (Londono and Hart 2013). The second and third detonations occurred at 12:40 pm on May 3 and 2:39 pm on May 5, respectively. These breaches were located at the southern edge of the front line levee and allowed for flood waters to return to the river channel. It was also reported that floodwaters stripped away soil from agricultural fields leaving behind scour marks, grooves, and potholes (Londono and Hart 2013).

3 Data and methods

3.1 Data

A 10-m (32.8 ft) digital elevation model (DEM) for the study area was obtained from the USGS National Elevation Dataset (NED). While the quality of the NED for flood modeling is variable depending on the source data (Sanders 2007), the DEM of the study area was created from an aerial lidar survey and published in 2013. The vertical accuracy is excellent, estimated to be less than 0.2 m (0.65 ft) root mean squared error (RMSE) at scales of 10 m (32.8 ft), although small-scale features such as narrow river levees may not be as accurately represented (Gesch et al. 2014). This limitation is addressed with spot heights of levees (Fig. 3) collected in 2007 with a vertical accuracy of 3.8 cm (1.5 in.) using geodetic grade GPS receivers (Flor et al. 2011). Additionally, since the DEM used to represent topography contained no bathymetric information, cross-sectional transect data for the main channel were obtained from the USACE. The along-channel spacing of measured cross sections was 0.5 mi (0.80 km) for the Upper Mississippi River, 7 mi (11 km) for the Ohio River, and 4 mi (6.5 km) for the lower Mississippi River.

The uneven cross-sectional distribution is due to the bathymetric features of the three river reaches. Within the modeling domain, the Ohio and Lower Mississippi Rivers exhibit average bed slopes of 0.0032 and 0.0079 %, respectively, and the fluctuations in bottom elevations are minimal for both reaches. However, the upper Mississippi River bed is

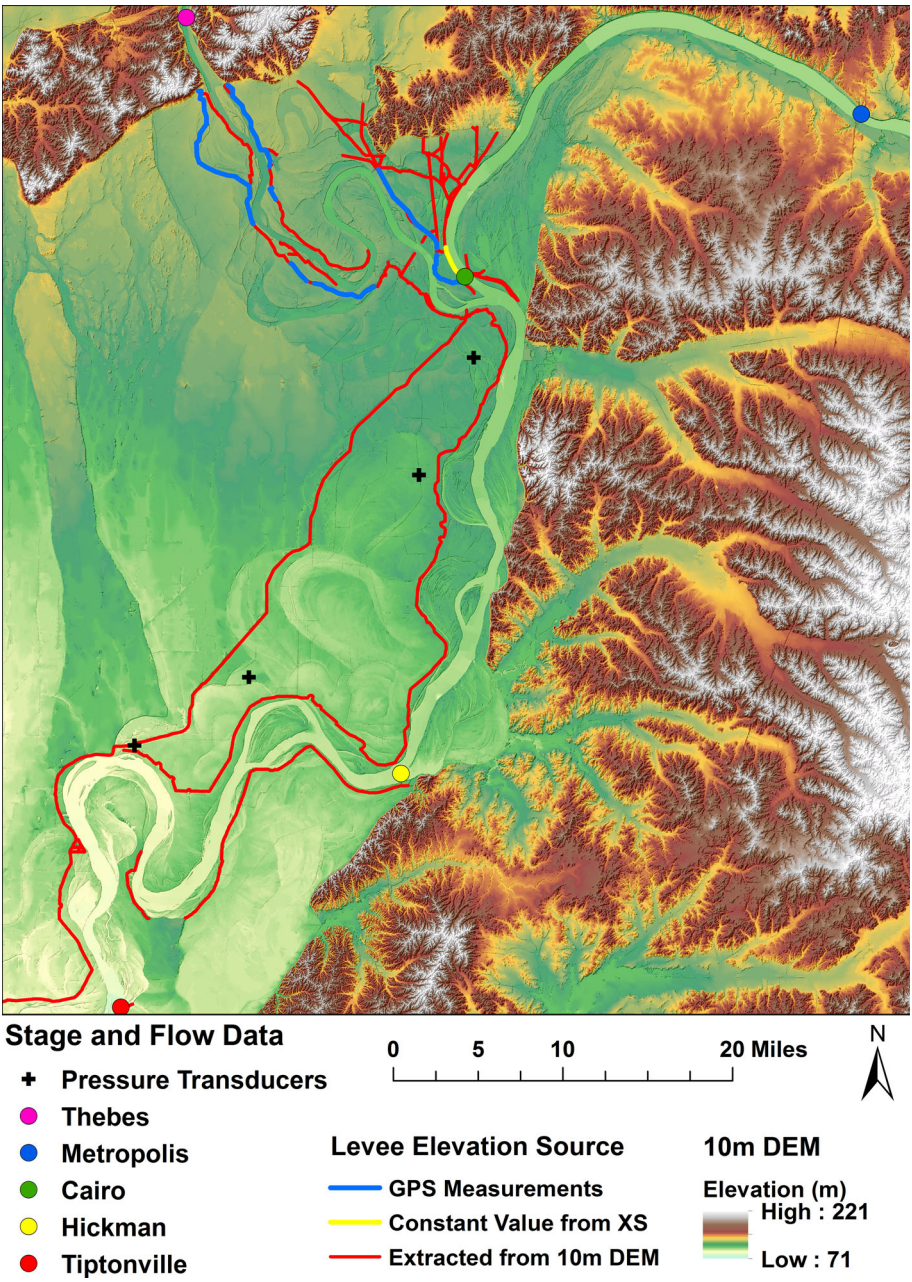

Fig. 3 Location of stage, flow, and levee elevation datasets

highly variable with a considerably steeper bed slope of 0.019 %, so more closely spaced cross sections were needed to accurately represent the bathymetry.

Discharge and stage measurements at USGS and USACE stream gages were used to parameterize and calibrate the flood model (Figs. 3, 4). Discharge and stage data were

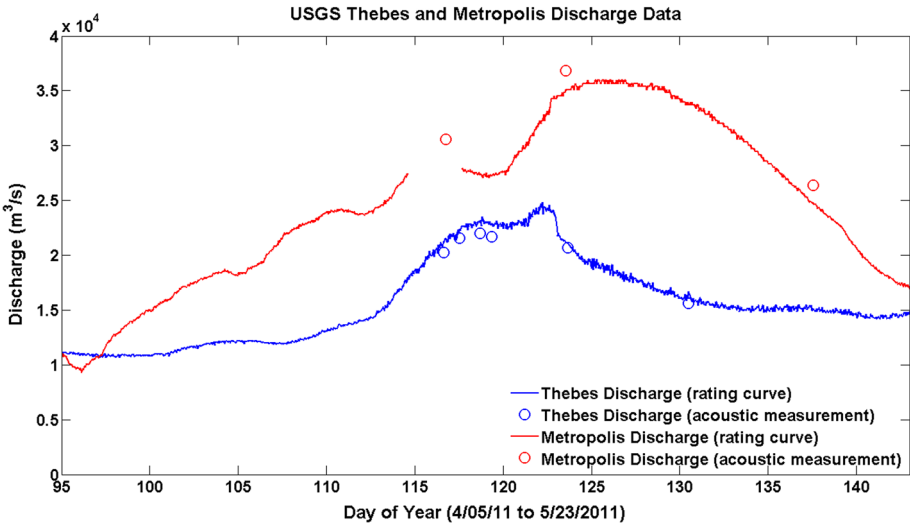

Fig. 4 Discharge data used to parameterize flow into the modeling domain

obtained from the USGS Ohio River gage at Metropolis, Illinois, and the USGS Mississippi River gage at Thebes, Illinois. Additionally, stage data were obtained from USACE gages at Cairo, Illinois; Hickman, Kentucky; and Tiptonville, Tennessee (Fig. 3). Stage values from the Tiptonville gage were used to define the water surface elevation at the downstream boundary of the model. Discharge data from the USGS gaging stations were calculated using a stage–discharge relationship, which are accurate to 5–10 % of actual flows at best (Hirsch and Costa 2004). However, since the stage–discharge relationship is calibrated during normal to high flows, the accuracy of the measurement is significantly diminished during flooding events due to the large amount of overbank flow. Because of this, USGS teams made flow measurements using acoustic technology at Metropolis and Thebes during the peak of the flood, which consisted of a main channel and overflow measurement. Overbank areas for both locations were large and difficult to measure (Koenig and Holmes Jr 2013). The error associated with the acoustic measuring device is 3 % if working correctly, and additional error is introduced depending on site conditions. Measurement quality is rated from excellent to poor, with excellent quality signifying no additional error, and poor quality signifying over 10 % additional error. Acoustic measurements taken at Metropolis and Thebes during the peak of the flood were rated as good (5 % error) to fair (8 % error), which introduce a total error of 8–11 % when also considering error introduced by the acoustic measuring device (Koenig and Holmes Jr 2013).

Prior to floodplain activation, USGS teams deployed submersible pressure transducers (SPTs) at 38 locations within the NMF to record the changes in floodway water surface elevations following the detonations. The water surface elevations recorded by the SPTs were used to calibrate the breach geometry of the first detonation and roughness coefficients within the floodway. Four of the SPTs were selected to illustrate the match between model output and observations following calibration (Fig. 3). These four SPTs were selected so that the spatial variation in model performance is adequately demonstrated throughout the NMF. The accuracy of the water surface elevations recorded by the SPTs is similar to the accuracy of the recorded elevation of the sensor, which ranged from 0.6 cm

(0.24 in.) to 15.6 cm (6.1 in.) throughout the 38 deployed SPTs (Koenig and Holmes Jr 2013).

A 30-m (98 ft) resolution land use map was obtained from the National Land Cover Database 2006 (NLCD 2006) to quantify flooding extent according to land use. NLCD classifies land use based on Landsat satellite data from 2006. Additionally, in order to quantitatively examine soil erosion from the flood, soil data for the NMF were obtained from the Web Soil Survey (WSS). WSS provides soil data produced by the National Cooperative Soil Survey and is operated by the USDA National Resource Conservation Service (NRCS).

To calibrate model predictions of flood extent, Moderate Resolution Imaging Spectroradiometer (MODIS) images of flood extent were obtained from NASA's Aqua satellite. MODIS is a 36-band spectroradiometer, which measures visible and infrared radiation to derive data products related to land surface cover. Differences in measured visible and infrared light are used to show contrast between water and land surfaces, where water surfaces are shown in varying shades of blue. Images of the NMF taken by MODIS on April 29 and May 4, 2011, were used to quantify observed flooding extent in the modeling domain. The MODIS imagery obtained was 250-m (820 ft) resolution: Clouds, water surfaces, and land surfaces were clearly discernible. Three distinct classes (clouds, land, and water) were estimated by first applying the ISO cluster unsupervised classification algorithm in ArcGIS (ESRI, Redlands, CA, USA). Then, clouds were reclassified as either land or water, depending upon which surface the cloud appeared to overlap. This method produced binary images of water surfaces and land cover on May 4 and April 29, and the agreement (F) between observed flooding extent (A) and predicted flooding extent (B) was calculated as shown in equation one.

$$F = \frac{A \cap B}{A \cup B} \tag{1}$$

Equation 1 was applied to LISFLOOD-FP output and MODIS Imagery for April 29 and May 4 at 4:00 pm. The calculated F statistic was used measure how well model predictions of flooding extent matched observations prior to detonation (April 29) and post-detonation (May 4). The degree of agreement indicated by F primarily influenced the adjustment uncertain levee heights. These dates were chosen for calibration purposes so that maximum flooding extent prior to activation and immediately following detonation was accurately predicted by the hydraulic flood model.

3.2 DEM modifications

The 10-m (32.8 ft) DEM was coarsened to 60-m (197 ft) resolution for input in the hydraulic flood model, LISFLOOD-FP, which operates at the resolution of the DEM. The resampling method used to coarsen the DEM was bilinear interpolation, which determines the new cell value based upon a weighted distance average of the four nearest input cell centers and will cause some smoothing of the data. The modeling domain was 98 km (60 mi) by 87 km (55 mi) in size, and at a resolution of 60 m (197 ft), the domain was represented by 2,397,320 cells. Even at 60-m (197 ft) resolution, the model configuration was at the upper limit of the computational resources available at the time of the study, considering that the duration of the flood was 48 days. This resolution was found to provide a good 2D representation of river and floodplain flows, including exchanges between the river and floodplain. Topographic gradients within the NMF and surrounding floodplain are relatively small, and abrupt changes in topography rarely occur within 60 m

(197 ft). Thus, we did not expect the coarsening of the DEM to negatively impact predictions of floodplain flows. Since the coarsening of the DEM to 60 m (197 ft) filtered out critical high and low points corresponding to levees and roads, respectively, additional processing of the DEM was performed. In particular, levee elevations were extracted from the 10-m (32.8 ft) resolution DEM and the maximum values were assigned to the overlapping cells in the 60-m (197 ft) DEM. The heights of several elevated streets were also extracted and assigned to the 60-m (197 ft) DEM. This method preserves levee crest elevations from the 10-m (32.8 ft) DEM in the 60-m (197 ft) DEM. GPS-measured levee crest elevations were assigned to cells when available, and the height of Cairo's eastern levee was set to a constant value obtained from USACE (2010) (Fig. 3).

The representation of channel bathymetry in the DEM aimed to preserve the stage–area relationship at flood stages. Hence, the channel bottom elevation was set equal to the cross-sectional average of channel transect data, and channel heights were linearly interpolated in the along-stream direction. This method creates a rectangular approximation of the river channel. Additional processing of the river channel was implemented to represent wing dams, which are dispersed throughout the Mississippi River to promote a single, deep thalweg during low flows and manage sediment transport during high flows. Wing dams are submerged during normal flow and extend roughly halfway across the channel. Additionally, sediment accumulates behind the wing dams. The wing dams effectively promote a compound channel configuration with a deep thalweg and one elevated channel bank. Channel cross section data were too sparse to delineate the effect of wing dams, so aerial images (Google Earth™) of the river collected at low flow were used instead. The spatial extent of the wing dams and accumulated sediment was manually delineated, and within these regions, the elevation was set equal to the original elevation provided by the 10-m resolution NED (Fig. 5). Based on these modifications, the channel geometry is represented through USACE transect data for the main, deepwater thalweg and the NED data where wing dams and accumulated sediment are present.

3.3 Hydraulic flood model

LISFLOOD-FP is a quasi-2D hydraulic flood model based on shallow-water theory that solves a 2D continuity equation and two 1D momentum equations to account for flow velocity (and discharge per unit width) in both the easterly (x) and northerly (y) directions (Bates et al. 2010; Neal et al. 2012). The momentum equations account for local accelerations, pressure gradients, and friction modeled in accordance with the Manning equation and are thus limited to unsteady, subcritical flows, which correspond to the vast majority of river flooding conditions (Neal et al. 2012). Supercritical flows are likely to occur in the moments following a levee detonation and may persist for a period of hours until backwater effects submerge the tailwater of the breach flow, so the LISFLOOD-FP predictions of depth and velocity locally around the breach are expected to have reduced accuracy during this time (Neal et al. 2012). However, LISFLOOD-FP will remain stable during the breaching process, so the model provides a reasonable approximation of the flow once the tailwater becomes subcritical. The reduced representation of local supercritical flow in the model does not appear to negatively impact far field predictions of flooding based upon comparisons of modeled stage with observed stage within the NMF. Moreover, computed Froude numbers within the NMF ranged between 0.2 and 0.8 eight hours following the levee detonation, which indicated that the breach and floodway flows quickly became subcritical. Floodplain velocities used in the analysis of inundated areas were only taken

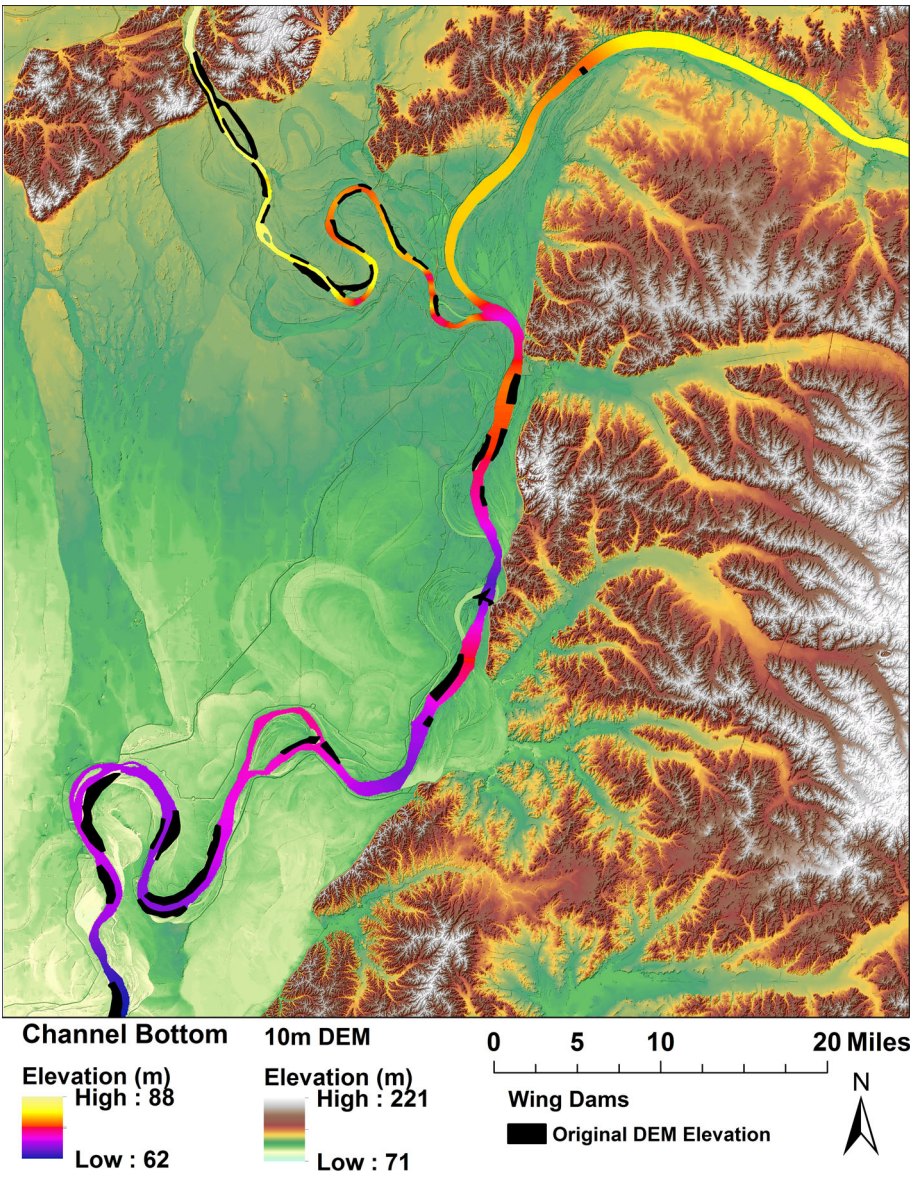

Fig. 5 Channel elevations and locations of wing dams

from model time steps after floodplain flows returned to subcritical states in order to avoid reduced accuracy associated with the supercritical flow limitations of the model.

3.4 Model setup and calibration

Flooding in the system was modeled starting at 8:00 am April 5 and ending at 8:00 am May 23. This extended simulation time (48 days) was chosen to capture the rise and fall of the hydrograph. In order to recreate the levee detonations, the simulation was paused at the

time of the first detonation. The DEM was then modified by lowering the levee elevations along the 3.2-km (2 mi) stretch of detonated levee at the northern fuseplug, and the simulation was continued using the modified DEM. This process was repeated for the second and third levee breaches.

Model calibration consisted of modifying Manning roughness coefficients, local levee crest elevations, input discharge at Metropolis, and the reduction of levee heights caused by detonation. The first step in the calibration procedure involved adjusting Manning n values within the channel and the directly adjacent floodplain (the riparian corridor) to match observations of stage at the USGS and USACE gaging stations. Manning n was adjusted so that the predicted water surface elevations matched observed water surface elevations during the days, leading up to the detonations, using the published rating curve discharges at Thebes and Metropolis to parameterize flow. A manual, iterative process was used, and final calibrated values were 0.031 $m^{-1/3}$ in the channel from Thebes to Cairo, 0.045 $m^{-1/3}$ in the channel from Metropolis to Tiptonville, and 0.06 $m^{-1/3}$ for the adjacent riparian corridor (Manning n values for the NMF were adjusted in a later calibration step). The floodplain Manning n value compares favorably with literature values for riparian corridors, and the Manning n values within the channel are within the range of appropriate values for natural rivers (Chow 1959). However, after the first 17 days of simulation (day of year 112), the model systematically under-predicted stage within the channel, despite matching observations during the lower flows of the first 17 days. Since the under-prediction could not be corrected by increasing Manning n values, and model predictions matched observations during the more certain lower flows, the systematic deviation after the first 17 days was attributed to errors in the input discharge. Thus, input discharge became a necessary calibration parameter.

Before adjusting the input discharge, errors in the elevations of levee crests were corrected. Since highly accurate spot heights of levees were limited, the majority of the levee heights were based on the 10-m (32.8 ft) NED, which may filter out local height maxima. This error typically manifests itself as a local low point on the levee, as much as 0.5 m (1.6 ft) below surrounding cells. In order to identify and remove these local low points, modeled flood extent was compared with the MODIS imaging of flood extent on April 29, and levee heights were raised to the elevation of surrounding cells where levee overtopping was observed in the modeled output but not observed in the MODIS imaging. Identifying errors in the levee elevations was fairly straightforward, since the local low points would cause levee overtopping that was not observed in MODIS imagery despite the under-prediction of river stage on April 29 at this point in model calibration.

After removing local low points in the levee system and calibrating Manning n values for the lower flows, the input discharge at Metropolis was adjusted to correct the systematic under-prediction of river stage following the first 17 days of the simulation. During this period of the flood, the rating curve discharge likely underestimates the true discharge due to the large amounts of overbank flow that begin to occur. This is confirmed by the acoustic measurements taken at Metropolis, which were all greater than the rating curve discharge values. The input discharge at Thebes was not adjusted, because acoustic measurements were more similar to the rating curve values (Fig. 4). Two additional input hydrographs were created for these high flow stages using a shape preserving interpolation between acoustic measurements and "shape points." Shape points are defined as discharge values that were created to preserve the shape of the rating curve hydrograph when interpolating between acoustic measurements. The values of shape points were obtained by adding the difference between the acoustic measurement and the rating curve discharge to a rating curve discharge at a nearby point in the hydrograph. This method was used to generate the

shape points at day of year 119 and 126 (Fig. 6). These points were created in order to represent the local low points and peaks of the hydrograph. Shape point values were also obtained by using acoustic measurements on the opposite side of the hydrograph. For example, the shape point value near day of year 114 is equal to the value of the acoustic measurement at day of year 137. The rating curve discharge at both of these points is also equal. This method was used to obtain the value of the shape point at day of year 130 and 114. Simulations using this generated hydrograph still under-predicted water surface elevations near Cairo, so a second hydrograph was created by increasing shape points and acoustic measurements by 4.5–7.0 % (Fig. 6). Shape points and acoustic measurements were increased by a higher percentage near the peak of the flood because the magnitude of error is likely to increase with increasing flows. Values of 4.5 and 7.0 % were chosen so that predicted water surface elevations immediately prior to the detonations matched observations closely at the Cairo gage. These percent increases are within the acoustic measurement's error range, and the adjustment to the discharge at Metropolis successfully corrected the under-predictions of stage during the high flows, leading up to the levee detonations. Therefore, the inflow discharge at Metropolis is based on interpolations between acoustic measurements and shape points plus 4.5–7.0 % from day of year 112 to 138 and published rating curve discharges from day of year 95 to 112 and 138 to 143.

The last step in the calibration procedure involved adjusting the Manning n value of the NMF and the height of the detonated levees. This calibration step was meant to ensure that the model is reasonably recreating the levee detonation and that predicted flow velocities across the floodplain are accurate. In reality, the cross-sectional area of a levee breach will evolve with time and typically grow as the breach flows erode the remaining levee structure. In the case of the NMF activation, a LiDAR survey of the floodway taken following the detonation shows that breach flows eventually eroded the levee crest to the height of the surrounding ground elevations (Londono and Hart 2013). However, it is difficult to determine the length of this process and the dimensions of the cross-sectional area immediately following the detonations. Initial simulations in which the sections of detonated levees were lowered to ground elevations resulted in a rapid under-prediction of

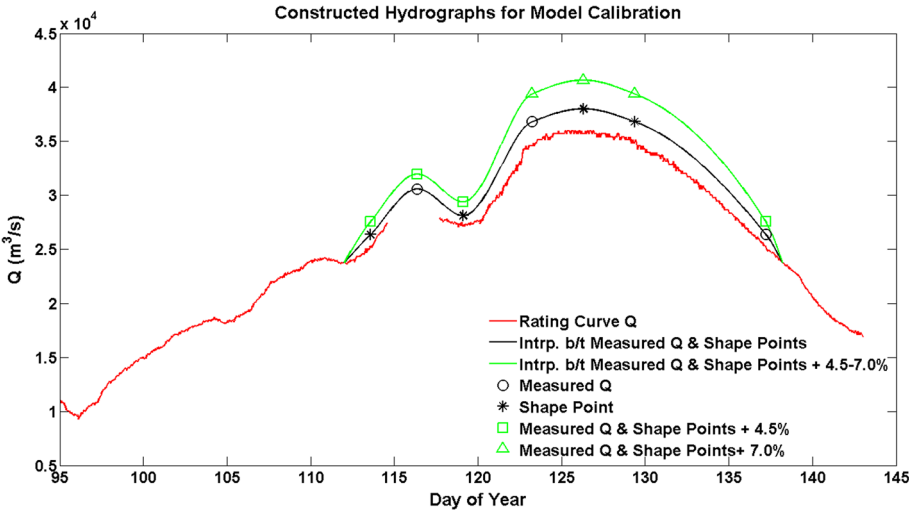

Fig. 6 Measured and constructed hydrographs at Metropolis

stage at Cairo and an over-prediction of stage at the PTSs deployed within the floodway. This indicated that the detonations did not immediately lower crest elevations to ground surfaces, and some levee structure remained that was eventually eroded. In order to improve the model's prediction of stage within the NMF and at the Cairo gaging station following detonation, another manual, iterative process was used to adjust the NMF Manning n value and initial reduction in levee heights caused by detonation. This process resulted in a Manning n value for the NMF of 0.04 $m^{-1/3}$ and detonated levee heights 2.0 m (6.56 ft) above surrounding ground elevations. These values were chosen to minimize the residuals between modeled and measured water surface elevations within the floodway and to closely match the reduction in stage observed at Cairo during the hours immediately following the breach. The reduction in stage immediately after detonation was prioritized for calibration because maximum flow velocities occurred during this time.

The calibrated model represents a hindcast of NMF flooding dynamics under the detonation control scenario that was implemented by USACE. To characterize flooding dynamics associated with a passive control scenario, which does not involve any levee detonations, LISFLOOD-FP was applied again using calibrated model parameters and only the initial DEM file that represents levees unaltered by explosive detonations. Otherwise, all input parameters were identical. Based on this configuration, the NMF will flood, but instead of water entering from the three detonation locations, the NMF fills from water naturally overtopping low points in the levee system (passive control).

3.5 Analysis of inundated areas

Flooded areas were measured in accordance with land cover by quantifying the maximum flood extent and overlaying the 2006 NLCD on the predicted flooding. Urban flooding is defined as the area of modeled flood extent which overlapped low-, medium-, and high-intensity development as defined by the 2006 NLCD legend (classes 22, 23, and 24). Agricultural flooding was also quantified and is defined as the area of modeled flood extent, which overlapped pasture/hay and cultivated crops (classes 81 and 82). Also, an index of flood erosion was estimated by measuring the areal extent of land that potentially experienced erosion in each of the two control scenarios. Based on the WSS data, 90 % of the soils within the NMF were classified as Sharkey or similar soil types. These soils have a particle distribution of roughly 75 % clay, 22 % silt, and 3 % sand (Pettry and Switzer 1996). According to this particle distribution, the average soil particle size within the NMF was estimated as 0.02 mm (0.04 in.) (ISO/IEC 2002), and according to the Hjulstrom curve, erosion will start to occur when water velocities reach 40 cm/s (12 in./s) for particles with a grain size of 0.02 mm (0.04 in.) (Hjulstrom 1935). Since the NMF is primarily used for agriculture, the majority of the floodplain was vegetated before the floodplain was activated. This increases the soil's resistance to erosion, so soils that experience velocities greater or equal to 40 cm/s within the NMF will not necessarily erode. Thus, areas in the NMF which experienced flood velocities that exceeded 40 cm/s following the activation of the floodway were classified as "potentially erodible."

3.6 Economic damage modeling

In addition to measuring flood impacts by land use and erosion potential, economic losses were estimated using HAZUS-MH (Scawthorn et al. 2006). HAZUS-MH is a model developed by the United States Federal Emergency Management Agency (FEMA) for

estimating potential losses from earthquake, floods, and hurricanes. Potential losses are based on the intensity of a natural hazard in affected census blocks. In flooding scenarios, depth–damage curves are used to determine the percent of total building value lost for particular flooding depths. Agricultural losses are estimated based upon crop type, the time that flooding occurred, and the duration of the flooding event. The HAZUS-MH software includes a default inventory database, which describes the count and value of structures within the study area based upon 2000 US Census data and Dun & Bradstreet Business Population Report. A library of depth–damage curves is also included in the software, which was compiled from studies conducted by various USACE districts and the Federal Insurance Administration. In this study, the default inventory database and depth–damage curves were used to estimate the economic losses associated with the depths predicted by LISFLOOD-FP for the passive and detonation control scenarios. Assumptions used in the application of HAZUS-MH include a warning time of 48 h and that inundation lasted 14 days over agricultural land. Also, a disaster scenario in which Cairo itself was inundated beneath 6 m (20 ft) of water was used to quantify the potential cost of the eastern Cairo levee failing. A depth of 6 m (20 ft) was chosen because this represents the depth obtained by subtracting Cairo's average land surface elevation from the water surface elevation in the Ohio River channel at the peak of the flood under the passive control.

Results reported from the economic damage analysis include the estimated direct economic losses for buildings and agricultural products. Direct economic loss for buildings consisted of depreciated capital losses (building and commercial inventories) and income losses (relocation, wages, and rental losses), while direct agricultural losses consisted of crop damages over the assumed inundation period of 14 days. Depreciated replacement values were reported for building losses since full replacement values likely overestimate the true losses (Merz et al. 2010). There is a high amount of uncertainty related to flood damage estimates in general (Merz et al. 2004; Meyer et al. 2013), which is primarily attributed to errors in the inventory value, the depth–damage curves, and flooding depths. Since default HAZUS-MH inventory values were used instead of appraisal data for the study area, the absolute values of the estimated damages must be viewed with caution. However, the damage estimates are still useful for assessing the relative damage between the detonation and passive control.

4 Results

The calibrated recreation of the detonation event compared reasonably well with both observed flooding extent and river stage. The calculated F statistic of 0.73 and 0.76 for April 29 and May 4 suggests that model predictions of flood extent agree with observations over roughly 70 % of the inundated area (Figs. 7, 8; Table 1). This 70 % agreement is similar to other successful model comparisons with remotely sensed flooding extents (Horritt and Bated 2001; Bates et al. 2006; Wilson et al. 2007). The 30 % disagreement can be attributed to several factors. Firstly, there are inundated areas captured by MODIS imagery that are not hydraulically connected to river reaches within the modeling domain. These areas are small lakes that are not connected to the floodplain and may be perennially flooded or seasonally flooded by rainfall or seepage. Secondly, disagreement can be attributed to errors in the relatively coarse representation of the levee system. In general, the modeled levee system worked to constrain floodwaters and simulate overtopping when appropriate. However, in several locations that appear to be protected by levees, MODIS

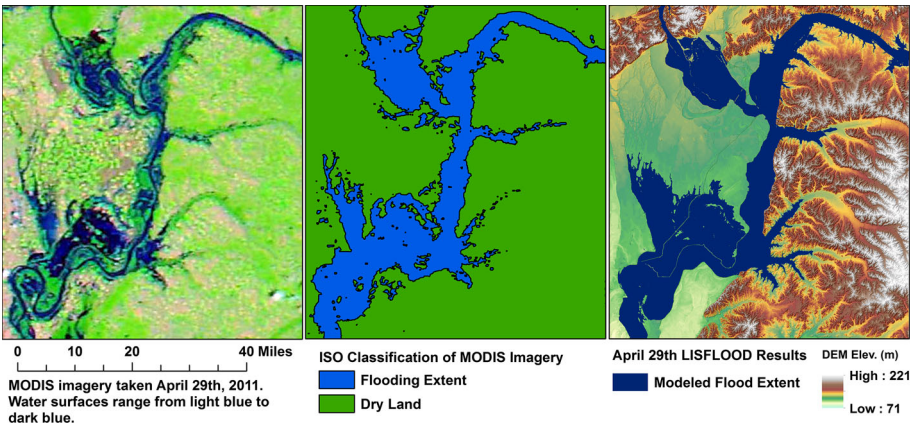

Fig. 7 MODIS imagery of flood extent (*left*), ISO unsupervised classification of MODIS imagery (*middle*), and predicted flood extent by LISFLOOD-FP on April 29 (*right*)

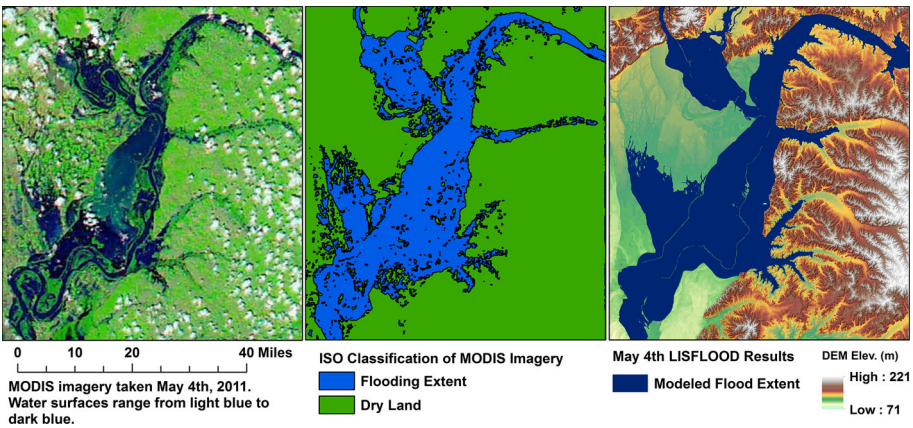

Fig. 8 MODIS imagery of flood extent (*left*), ISO unsupervised classification of MODIS imagery (*middle*), and predicted flood extent by LISFLOOD-FP on May 4 (*right*)

imagery shows inundated floodplain where modeling results do not predict flooding (Figs. 8, 9). This error can be attributed to inaccuracies in the heights of the modeled levee system, seepage under levees which were not accounted for, or culverts beneath levees that were not discernible in aerial imagery. Thirdly, disagreement could be caused by errors in the unsupervised classification scheme, which tended to over classify flooding extent at the interface of land and water surfaces due to the coarseness of the MODIS imagery. Lastly, lateral inflows tributary to the floodplain emanating from small catchments within the modeling domain were not parameterized in the model. These flows were not measured and likely contribute to the under-prediction of flooding extent observed on May 4 (Table 1).

Modeled stage values exhibited a RMSE of just 0.30 m (0.99 ft) when averaged between the five gaging stations (Fig. 9; Table 2). The match between the modeled and

Table 1 Comparison between modeled and observed flooding extent

	Flood extent, MODIS classification	Flood extent, model prediction	MODIS ∩ model	*F* statistic
April 29th, 2011	190,115 ha (469,784 ac)	191,310 ha (472,737 ac)	159,750 ha (394,751 ac)	0.73
May 4th, 2011	231,163 ha (571,215 ac)	227,820 ha (562,955 ac)	196,060 ha (484,474 ac)	0.76

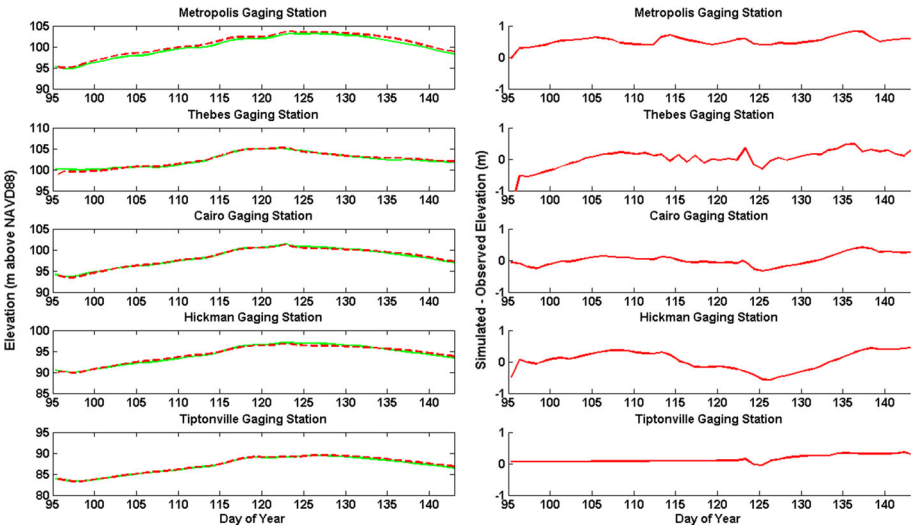

Fig. 9 Simulated stage (*red dotted lines* in the *left panels*) compared with observed stage (*solid green lines* in the *left panels*) and the difference between simulated and observed stage (*five panels* on the *right*)

Table 2 Simulated stage error statistics by gaging station

	Root mean squared error	Mean absolute error	Absolute error at peak stage
Thebes	0.33 m (1.08 ft)	0.22 m (0.72 ft)	0.03 m (0.09 ft)
Metropolis	0.53 m (1.73 ft)	0.51 m (1.70 ft)	0.58 m (1.90 ft)
Cairo	0.18 m (0.60 ft)	0.14 m (0.45 ft)	0.02 m (0.06 ft)
Hickman	0.30 m (0.98 ft)	0.26 m (0.85 ft)	0.31 m (1.01 ft)
Tiptonville	0.18 m (0.60 ft)	0.15 m (0.49 ft)	0.10 m (0.33 ft)
Gaging station mean	0.30 m (0.98 ft)	0.25 m (0.84 ft)	0.20 m (0.68 ft)

observed stage is likely near the maximum fit achievable given the estimated RMSE of 0.20 m (0.65 ft) in the elevation data. The lowest mean absolute errors of 0.14 m (0.45 ft) and 0.15 m (0.49 ft) are observed at the Cairo and Tiptonville gages, respectively. Tiptonville is closest to the downstream boundary, where observed water surface elevations were used to define the elevation at that boundary, so it is expected that modeled stage would closely match observation. To ensure water surface elevations were particularly

accurate in the center of the modeling domain, the accuracy of stage at Cairo was prioritized during model calibration at the cost of stage accuracy for gages near the modeling domain border. Notice that the absolute error at peak stage is just 0.02 m (0.06 ft) for the Cairo gage, indicating that water surface elevations near the detonation location are particularly accurate prior to activation. Model accuracy is most important at peak stage, since maximum flood depths used in the analysis of inundated areas occur at this time. The largest mean absolute error of 0.51 m (1.70 ft) occurs at the Metropolis gage, which can be attributed to the uncertainty of the input discharge near the peak of the flood. The biggest difference between predicted and observed stage (about 0.4 m) occurs around day of year 125 (May 5) for the Cairo, Hickman, and Tiptonville gages. This is most likely due to the complex flows and stage changes associated with the levee detonations.

Roughly 10 h following the detonation of the northern fuseplug levee, observations at the Cairo gage show that stage prior to detonation was reduced by 0.36 m (1.2 ft), while modeling results predict a 0.40 m (1.3 ft) reduction in stage (Fig. 10). The similarity between the observed and modeled stage reduction suggests that the modeled breach discharge is particularly accurate soon after the breach. Moreover, the rapid reduction in stage that is recorded at Cairo confirms the effectiveness of the levee detonation from a flood stage reduction perspective. The accuracy of Cairo flood stage predictions slightly decrease after the first 10 h of the simulated breach. Since modeled stage within the NMF is highly accurate during the initial hours of the breach and thereafter (Fig. 11), exhibiting a mean RMSE of only 0.16 m (0.52 ft) when averaged between 38 SPTs, the flow physics and breach geometry appear adequately represented. This suggests that the error in flood stage during the falling limb is likely due to uncertain inflows associated with smaller catchments tributary to the flood zone which were not considered in the model. These flows are extremely difficult to characterize because they were not measured, and it is unlikely that the missing discharge emanates from the Ohio River since modeled stage is slightly high at the Metropolis gage (Fig. 9). Another potentially important factor is that the breach

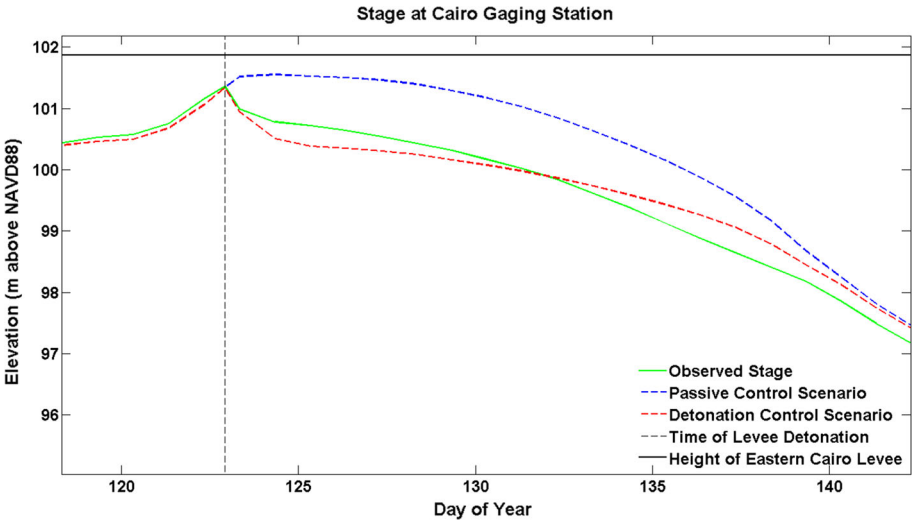

Fig. 10 Stage changes at the Cairo gaging station under the detonation and passive control scenarios. The time of the levee detonation and height of the eastern Cairo levee are shown for reference

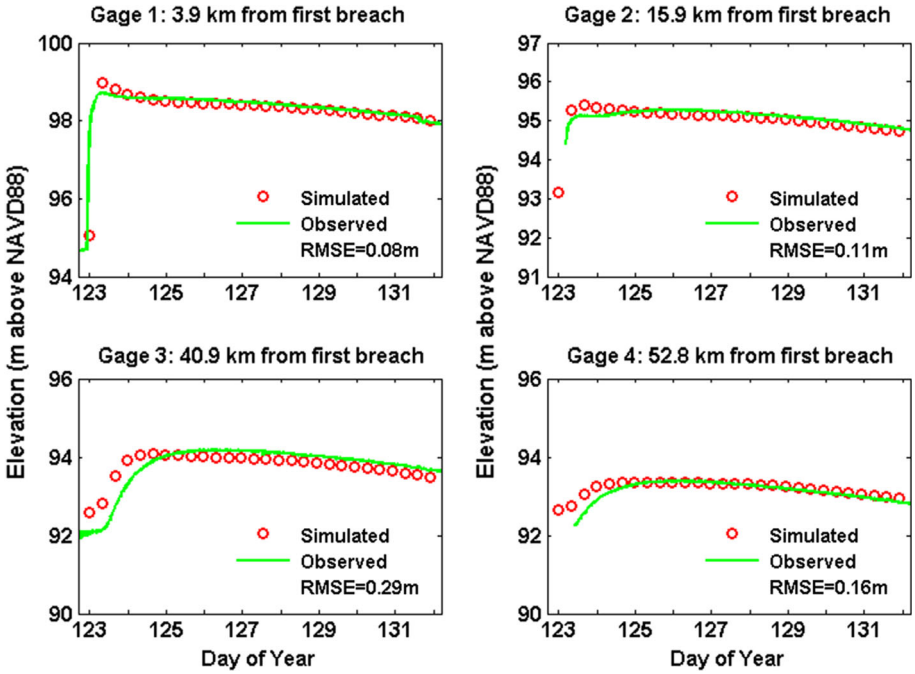

Fig. 11 Comparison of simulated and observed stage within the NMF following detonation. Refer to Fig. 3 for location of gages (pressure transducers within floodway)

geometry evolved following detonation, as high-velocity flows deepened and possibly widened the breach. In the model, the breach shape is assumed constant. Additional modeling to correct stage errors on the receding limb of the hydrograph was deemed unnecessary because maximum depths and velocities occur within 36 h of the levee detonations, and modeled stage compares favorably with observations within the NMF (Fig. 11). The accuracy of the model at peak flood stages and within the NMF provides confidence in the model predictions of maximum flood depths and velocities used in analysis of inundated areas. However, the uncertainty in the input discharge and lateral floodplain inflows is a considerable limitation of this study, especially with respect to stage changes associated with the passive scenario.

The detonation of the upper fuseplug levee appears to have been well timed in two aspects based on previous breach design research (Jaffe and Sanders 2001; Sanders et al. 2006). Firstly, when the diversion site is downstream of the protection site, as is the case here, it is important to allow adequate time for depression waves to travel upstream and reach the protection site prior to the flood peak. Since the northern fuseplug levees are only several kilometers downstream of Cairo, depression waves moving upstream from the diversion location arrived at Cairo with stage lowering capacity in a matter of minutes, well before the arrival of the peak flood stage. Secondly, in order to maximize the flood stage reduction effect of the breach flow, the peak diversion rates must be sustained through the passing of the flood peak. If the flood peak is assumed to occur on day of year 125, which was when the maximum discharge was recorded on the Ohio River (Fig. 4), then the detonation occurred roughly 2 days prior to the flood peak. USGS measurements

and model predictions of breach flows show that breach discharges fluctuated between 11,470 m^3/s (405,000 ft^3/s) and 10,190 m^3/s (360,000 ft^3/s) before sharply declining on day of year 128, or May 8, 2011 (Koenig and Holmes Jr 2013). Since peak breach discharges did not significantly decline until after the passing of the flood peak, the timing of the detonation likely occurred within a several day window that could be considered optimal from a stage reduction perspective. Cairo's proximity to the breach location and the sustained peak diversion flows suggest that optimal NMF performance from a stage reduction perspective can be achieved through detonation within roughly 5 days of the flood peak, which was the case during the 2011 activation.

Comparison between the passive control peak stage and observed peak stage shows that stage at Cairo would have increased by approximately 0.21 m (0.69 ft) before receding had the fuseplug levees not been detonated (Fig. 10). While the 0.21 m (0.69 ft) rise in stage only corresponds to a 1 % increase in depth, a 1 % increase in depth increases the hydrostatic force acting on the Cairo levees by 2 % or 44 kN (9892 lbs) per unit width. Moreover, Fig. 10 shows that detonation resulted in a sustained reduction of stage on the order of 0.8 m (2.62 ft) that lasted over a period of roughly 2 weeks. Although the model did not predict any overtopping of the levees surrounding Cairo in the passive control scenario, the water surface elevation was within 0.34 m (1.1 ft) of the eastern levee crest. Due to the high amount of uncertainty in the input discharge during the peak flood stages, it is not possible to conclude whether the eastern levee at Cairo would have overtopped had the fuseplug levees been left intact. Nevertheless, the increased hydrostatic force acting over a period of 2 weeks and the small amount of freeboard in the passive control scenario point to a much higher risk of levee failure than under the detonation scenario. Furthermore, the passive control scenario reveals overtopping of levees within the modeling domain other than the eastern levee crest at Cairo (Fig. 12).

In the passive control scenario, floodwaters overtopped the fuseplug levee (activating NMF passively) and levees protecting Mound City, IL, which is just north of Cairo. This suggests that with or without detonation, the NMF would have become inundated. Levee overtopping caused the maximum flood extent to be slightly greater in the passive control

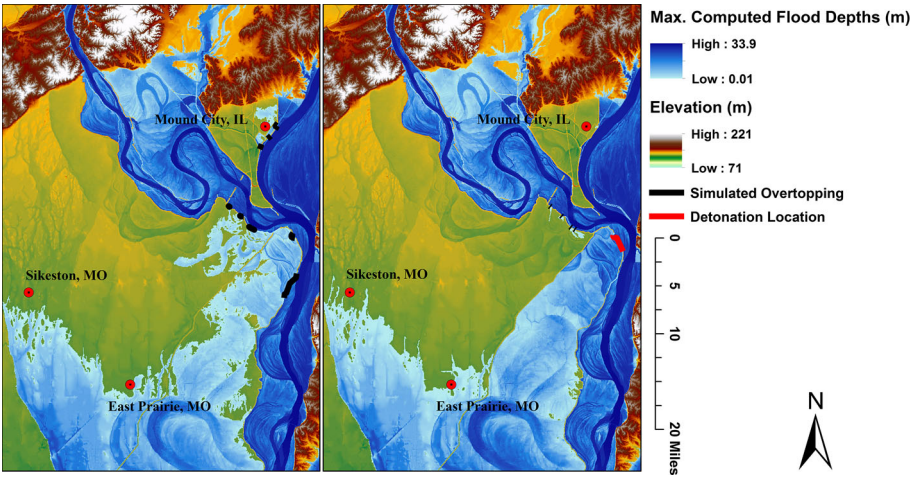

Fig. 12 Maximum flood depths near Cairo in the passive control scenario (*left*) compared with maximum flood extent near Cairo in the detonation control scenario (*right*)

scenario (Table 3). In the detonation control scenario, flood waters exiting the NMF spill into the floodplain north of the lower fuseplug, causing further reaching flooding extent around Sikeston and East Prairie, MO (Fig. 12). This caused the total area of urban and agricultural flooding to be slightly greater under the detonation control scenario (Table 3). While the agricultural and urban area of flooding is comparable between the two scenarios, results show that the potentially erodible floodway area is 3900 % greater under the detonation control scenario (Table 3, Fig. 13). Breach flows following detonation exceeded the estimated threshold of damaging flow velocities across 47 % of the floodway. Under the passive control scenario, water was predicted to move more slowly across the floodway causing minimal erosion.

Application of the HAZUS-MH model (Table 4) indicates damages exceeding 250 million US$ under both scenarios based on agricultural and building losses, and surprisingly, damages based on the detonation scenario are estimated to be 11 million US$ less than the passive control scenario. Most of the mitigated losses are related to building

Table 3 Classification of inundated areas (percentage change is relative to the passive control)

	Total inundated area	Area of urban flooding	Area of agricultural flooding	Erodible floodway area
Detonation control	232,220 ha (573,828 ac)	1833 ha (4529 ac)	127,310 ha (314,589 ac)	25,486 ha (62,977 ac)
Passive control	232,370 ha (574,198 ac)	1780 ha (4398 ac)[a]	126,960 ha (313,724 ac)	636 ha (1571 ac)
Percentage change	−0.06	+3.0	+0.3	+3900

[a] The failure of Cairo's eastern levee would have caused an additional 352 ha (870 ac) of urban flooding

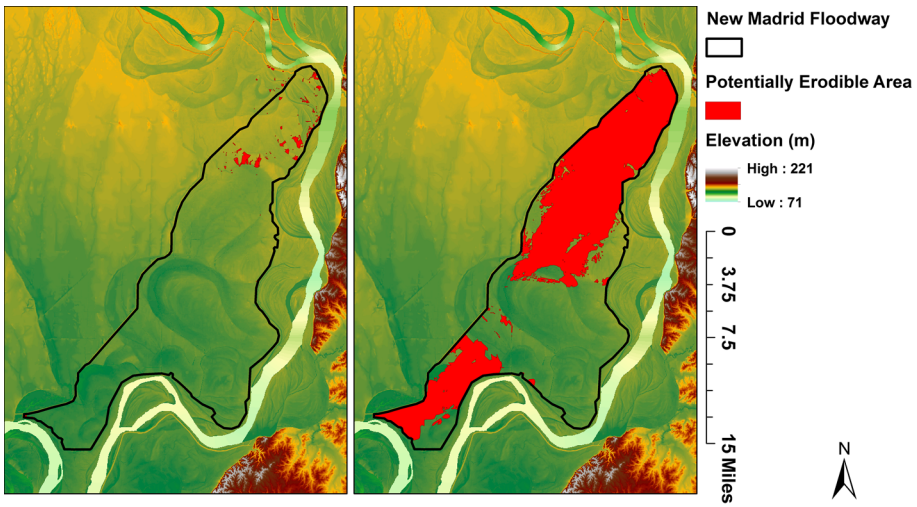

Fig. 13 Potentially erodible soils of the passive control scenario (*left*) compared with potentially erodible soils of the detonation scenario (*right*)

Table 4 Economic loss estimates (percentage change is relative to the passive control)

	Direct agricultural losses	Direct building losses	Ag. + building losses
Detonation control	92,330,730 US$	179,434,000 US$	271,764,730 US$
Passive control	93,820,220 US$	189,258,000 US$[a]	283,078,220 US$
Percentage change	−1.6	−5.0	−4.0

[a] The failure of Cairo's eastern levee would have caused an additional 90,793,000 US$ in estimated building losses

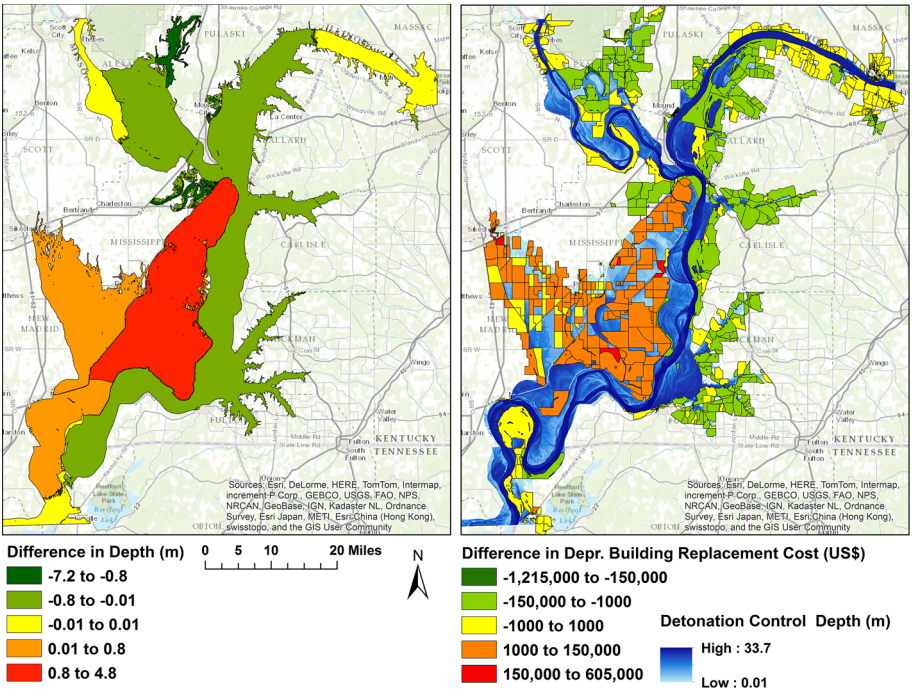

Fig. 14 Detonation control minus passive control maximum flood depths (*left*) compared with detonation control minus passive control building replacement costs by census block (*right*). *Green areas* indicate a decrease in flood depths or building replacement costs caused by the detonation, while *orange/red* areas indicate that flooding depths or building replacement costs were increased by the detonation relative to the passive control. The *color scales* are nonlinear to emphasize extents of areas that were more drastically affected

replacement costs, since agricultural losses are similar between the two scenarios. The reduced building losses under the detonation scenario can be attributed to the stage reduction achieved upstream of the detonation locations. This is illustrated in Fig. 14, where census blocks within areas upstream of the detonation locations are shown to sustain lower building replacement costs. Under the passive control scenario, deeper and further reaching flood waters extend to areas upstream of the detonation locations, causing increased building damages. Reductions in channel flood stage upstream of the levee detonations are consistent with subcritical channel flow hydraulics, because depression waves move in

both the upstream and downstream directions (Sanders and Katopodes 1999a, b). As expected, the detonation caused deeper flood depths and more building damages within the NMF and downstream floodplain areas compared with the passive control (Fig. 14). Under the passive control scenario, if levees at Cairo had failed and flood heights equalized with the peak stage in the river channel, the estimated building replacement costs at Cairo would have been 90.8 million US$, increasing losses associated with the passive control scenario by 32 %.

5 Discussion

The detonation control was designed principally to reduce flood risk at Cairo, and this goal was clearly achieved based on the reduction in flood stage upstream of the detonation point and the stability of the levee system guarding the city (Figs. 10, 14). Reducing the risk of Cairo levee failures was undoubtedly an important objective, as indicated by the relatively high cost associated with levee failure in Table 4. Although results show that detonation caused an estimated 0.06 % reduction in overall flooding extent and a 4.0 % reduction in agricultural and building losses, these percent changes are not especially significant due to the errors associated with the predicted flooding extent and economic damage modeling, respectively. The important conclusion that can be made is that detonation did not significantly *increase* flooding extent, building losses, or agricultural losses because passive overtopping of the levee system would have led to similar flooding extent and damages. Thus, the detonation successfully reduced upstream flooding depths and the risk of levee failures at Cairo without causing a significant increase in building and crop losses. These factors collectively suggest that the hydraulic controls implemented in the NMF were successful. However, there is one significant drawback that deserves consideration: the cost of floodplain erosion and deposition associated with the detonation and high-velocity dam-break-type flows, which were not considered in the HAZUS-MH damage model. Olson and Morton (2013) report that the USACE received 22 million US$ to restore the levees and fill scour holes adjacent to the detonation site and an additional 35 million US$ were allocated to remove sediment deposits from the NMF. Further, Olson and Morton (2013) report that the deposition of deltaic sands within the NMF will cause the previously finer-grained soils to be less productive. Under the passive control scenario, these damages would have been significantly reduced, as shown by the reduction in potentially erodible soils in Fig. 13. When comparing the potentially erodible floodway area between the two scenarios, the potentially erodible area should be viewed as areas within the floodway where flow velocities were predicted to exceed a damaging threshold. While the determination of the velocity threshold is somewhat simplistic, and based only on the particle size distribution within the floodway and the Hjulstrom curve (Hjulstrom 1935), the floodway velocities can be viewed with confidence due to the model's accurate reproduction of stage within the floodway (Fig. 11). Thus, we can definitively conclude that floodplain flows associated with detonation were significantly faster than flows associated with the passive control, and these faster flow velocities greatly increased floodplain erosion.

While it may be tempting to compare the 57 million US$ cost associated with floodplain repairs with the estimated 11 million US$ saved from Table 4, this comparison is not meaningful due to the uncertainties associated with the loss estimates. Ding et al. (2008) compared the default HAZUS-MH building inventory with appraisal data for a site in Houston, TX, and showed that the total inventory value estimated by HAZUS-MH was

65 % greater than the inventory values estimated through appraisal. Because the damages estimated by HAZUS-MH are essentially calculated as a percentage of the total inventory values, errors in the damage estimates are directly proportional to errors in the total inventory value. Consequently, errors in the absolute values of the damage estimates reported herein are expected to be on the order of 65 %. However, the relative damages between the passive and detonation scenarios are somewhat insensitive to updated inventory values, since an updated inventory would be exposed to the same depth–damage curves and flooding scenarios. Thus, the economic damage estimates from HAZUS-MH should be used to compare the relative costs of the detonation versus passive control, and not viewed in an absolute sense (Fig. 14). In order to compare HAZUS-MH damage estimates with the real costs of the detonation, the default inventory data would need to be updated with appraisal data for the modeling domain, which is outside the scope of this study.

On the subject of riverine flood control in general, the results from this study can be used to illustrate the advantages of rapid and passive floodway activation designs. In the case of a rapid activation, significant reduction in upstream flood stage is achievable at the cost of high-velocity breach flows. In the case of passive activation, minimal reductions in flood stage are achieved with greatly diminished floodplain velocities. Depending on the location, either approach could be deemed more appropriate based upon the perceived value of the upstream assets and the floodplain use. However, deciding whether to protect a floodplain or upstream properties will be necessarily controversial, due to conflicting opinions about ecological, social, and economic worth. An improved floodway activation technique which maximizes reduction in upstream stage while minimizing breach velocities would spare policy makers from deciding which asset to protect, while also improving the overall damage mitigation achieved through floodway activation. Designing such an activation technique would be particularly difficult, because minimizing breach velocities and maximizing stage reductions are conflicting objectives. Future studies which determine ideal breach geometries and floodway activation techniques by applying optimization methods to hydraulic modeling scenarios could be especially useful for the NMF and other floodways that rely on dam-break-type diversions of water into the floodplain.

6 Conclusions

The activation of the NMF with an explosive detonation scheme at specially designed fuseplug levees resulted in channel flood stages that were approximately 0.8 m (2.62 ft) lower than would have otherwise occurred under a passive control scenario where the levees remained intact. Further, the detonation had a lasting impact, whereby reduced channel stages on the order of 0.8 m (2.62 ft) lower persisted for over 2 weeks. The sustained reduction in flood stage and associated hydrostatic pressure led to greatly reduced risk of levee failures compared with a passive control approach. Surprisingly, the detonation scheme resulted in a slightly smaller areal extent of inundation (0.06 % reduction) and reduced losses associated with crop damages and building replacement costs (4.0 % reduction). While these percent reductions are not especially significant due to the errors in the hydraulic and damage modeling, the import result is that detonation did not significantly increase flooding extent, building, and crop damages compared with a passive approach. However, the detonation scenario produced damaging, high-velocity floodplain flows (scour holes and sandy soil deposits) requiring over 50 million US$ in repairs and the

likelihood of future losses in field productivity. Under the passive control scenario, the floodplain damages would have been greatly reduced. These results indicate that detonation resulted in substantially reduced risk of levee failures at Cairo without increasing overall flooding extent, building losses, and crop damages, but the potential for floodplain erosion and sediment deposition deserves additional consideration in the design of engineered floodways.

Acknowledgments This project was made possible by funding from the National Science Foundation (DMS-1331611) and The Ohio State University's Climate Water and Carbon program whose support is gratefully acknowledged. The authors also thank the United States Geological Survey and United States Army Corps of Engineers for providing data essential to this study. Lastly, the authors are thankful for the insights from reviewers which significantly improved the quality of this study.

References

Bates PD, Wilson MD, Horrit MS, Mason D, Holden N, Currie A (2006) Reach scale floodplain inundation dynamics observed using airborne synthetic aperture radar imagery: data analysis and modeling. J Hydrol 328:306–318

Bates PD, Horritt MS, Fewtrell TJ (2010) A simple inertial formulation of the shallow water equations for efficient two-dimensional flood inundation modeling. J Hydrol 387(1–2):33–45

Chow VT (1959) Open-channel hydraulics. McGraw-Hill, New York

Ding A, White JF, Ullman PW, Fashokun AO (2008) Evaluation of HAZUS-MH flood model with local data and other program. Nat Hazards Rev 9(1):20–28

Ernst J, Dewals BJ, Detrembleur S, Archambeau P, Erpicum S, Pirotton M (2010) Micro-scale flood risk analysis based on detailed 2D hydraulic modeling and high resolution geographic data. Nat Hazards 55:181–209

Flor A, Pinter N, Remo JWF (2011) The ups and downs of levees: GPS-based change detection, Middle Mississippi River, USA. Geology 39(1):55–58

Gesch DB, Michael JO, Evans GA (2014) Accuracy assessment of the US Geological Survey National Elevation Dataset, and comparison with other large-area elevation datasets-SRTM and ASTER. US Geological Survey Open-File Report 2014-1008. doi:10.3133/ofr20141008. Accessed 1 July 2014

Hirsch RM, Costa JE (2004) US stream flow measurement and data dissemination improve. EOS 85(21):197–203

Hjulstrom F (1935) Studies of the morphological activity as illustrated by the River Fyris: inaugural dissertation. Dissertation, Uppsala University

Horritt MS, Bated PD (2001) Effects of spatial resolution on a raster based model of flood flow. J Hydrol 253:239–249

ISO/IEC (2002) Geotechnical investigation and testing—identification and classification of soil—Part 1: Identification and description. ISO/IEC 14688-1

Jaffe DA, Sanders BF (2001) Engineered levee breaches for flood mitigation. ASCE J Hydraul Eng 127(6):471–479

Jongman B, Ward PJ, Aerts JCJH (2012) Global exposure to river and coastal flooding: long term trends and changes. Glob Environ Change 22:823–835. doi:10.1016/j.gloenvcha.2012.07.004

Kelley R (1998) Battling the inland sea: floods, public policy, and the Sacramento Valley. University of California Press, Oakland

Koenig TA, Holmes RR Jr (2013) Documenting the stages and streamflows associated with the 2011 activation of the New Madrid Floodway, Missouri. U.S. Geological Survey Professional Paper 1798-E. http://pubs.usgs.gov/pp/1798e/. Accessed 27 April 2013

Londono AC, Hart ML (2013) Landscape response to the intentional use of the Birds Point New Madrid Floodway on May, 3 2011. J Hydrol 489(1):135–147

Merz B, Kreibich H, Thieken A, Schmidtke R (2004) Estimation of uncertainty of direct monetary flood damage to buildings. Nat Hazards Earth Syst Sci 4(1):153–163

Merz B, Kreibich H, Schwarze R, Thieken A (2010) Assessment of economic flood damage. Nat Hazards Earth Syst Sci 10(1):1697–1724

Meyer V, Becker N, Markantonis V, Schwarze R, van den Bergh JCJM, Bouwer LM, Bubeck P, Ciavola P, Genovese E, Green C, Hallegatte S, Kreibich H, Lequeux Q, Logar I, Papyrakis E, Pfurtscheller C,

Poussin J, Przyluski V, Thieken AH, Viavattene C (2013) Review article: Assessing the costs of natural hazards—state of art and knowledge gaps. Nat Hazards Earth Syst Sci 13(1):1351–1373

Neal J, Villanueva I, Wright N, Willis T, Fewtrell T, Bates P (2012) How much physical complexity is needed to model flood inundation? Hydrol Processes 26(15):2264–2282

Olson KR, Morton LW (2013) Restoration of the 2011 flood-damages Birds Point—New Madrid Floodway. J Soil Water Conserv 68(1):13–18

Pettry DE, Switzer RE (1996) Sharkey soils in Mississippi. Mississippi State University Division of Agriculture, Forestry, and Veterinary Medicine Bulletin 1057. http://msucares.com/pubs/bulletins/b1057.htm. Accessed 4 July 2014

Sanders BF (2007) Evaluation of on-line DEMs for flood inundation modeling. Adv Water Resour 30(8):1831–1843

Sanders BF, Katopodes ND (1999a) Active flood hazard mitigation, Part 1: Bidirectional wave control. ASCE J Hydraul Eng 125(10):1057–1070

Sanders BF, Katopodes ND (1999b) Active flood hazard mitigation, Part 2: Omnidirectional wave control. ASCE J Hydraul Eng 125(10):1071–1083

Sanders BF, Katopodes ND (2000) Sensitivity analysis of shallow-water flow by adjoint method. ASCE J Eng Mech 125(10):1071–1083

Sanders BF, Pau J, Jaffe DA (2006) Passive and active control of diversions to an off-line reservoir for flood stage reduction. Adv Water Resour 29(6):861–871

Scawthorn C, Flores P, Blais N, Seligson H, Tate E, Chang S, Mifflin E, Thomas W, Murphy J, Jones C, Lawrence M (2006) HAZUS-MH flood loss estimation methodology II: Damage and loss assessment. Nat Hazards Rev 7(2):72–81

Sommer T, Harrell B, Nobriga M, Brown R, Moyle P, Kimmerer W, Schemel L (2001) California's Yolo Bypass: evidence that flood control can be compatible with fisheries, wetlands, wildlife, and agriculture. Fisheries 26(8):6–16. doi:10.1577/1548-8446(2001)026<0006:CYB>2.0.CO;2

United States Army Corp of Engineers (2010) The Mississippi River and tributaries project: Birds Point New Madrid project. http://www.mvd.usace.army.mil/Portals/52/docs/Birds%20Point-New%20Madrid%20info%20paper%20FINAL%200426.pdf. Accessed 4 May 2013

Wilson MD, Bates PD, Alsdorf D, Forsberg B, Horritt M, Melack J, Frappart F, Famiglietti J (2007) Modeling large-scale inundation of Amazonian seasonally flooded wetlands. Geophys Res Lett 34, paper no. L15404